

# Control of Power Flows in Low Voltage Distribution Systems

DARIO DE SANTIS, GAETANO ABBATANTUONO, SERGIO BRUNO, MASSIMO LA SCALA,  
ROBERTO SBRIZZAI

Dipartimento di Ingegneria Elettrica e dell'Informazione

Politecnico di Bari

Via Orabona, 4 - Bari

ITALY

dario.desantis@poliba.it; gaetano.abbatantuono@poliba.it; sergio.bruno@poliba.it;

massimo.lascalas@poliba.it

*Abstract:* - Electric distribution systems are undergoing many radical transformations, mostly driven by the deep diffusion of modern distributed generation units. This phenomenon asks for smart and highly optimized technical solutions, in order to deal aging infrastructures with better operational efficiency levels and assure the perfect management of electric networks and in particular for low voltage grids. In this paper, a methodology to reach fast and efficient power flow control and optimization on low voltage distribution systems through the installation of a unified power flow controller (UPFC) is presented. The numerical results of tests that have been carried out through different operating scenarios demonstrate how this device can be successfully applied also to these kind of electric networks, in order to solve common operational problems such as power losses, loop-flows and counterflows.

*Key-Words:* - distributed generation optimization, loss reduction, low voltage distribution grids, unified power flow controller

## 1 Introduction

In recent years, electric systems are turning into modern smart grids: this means that medium and low voltage (MV/LV) networks are becoming active grids, because of the always increasing presence of distributed generation (DG) units. Because of their power generation capability, these devices (PV panels, micro wind generators and so on) have transformed many ordinary electric users into prosumers who can either satisfy their own needs for electric energy or sell exceeding power generation to Distribution System Operators (DSOs) in charge of managing MV and LV grids. Unfortunately, this upgrading process is also causing many challenges that current aging distribution networks are often still not technologically ready to bear [1-8].

To a certain extent, DG units can increase power security, as long as they can provide power resources for voltage and power factor control. Nevertheless, a wide penetration of DG may lead to violations of minimum and maximum voltage constraints due to the bidirectional power flows. A further problem is given by the presence of power electronics converters that release current and voltage harmonics on the network.

Power quality and system security can also be worsened by the fact that DG units are not restricted by the regulations of the grid operator to maintain

system frequency: this leads to an impact also on global efficiency and emissions levels.

The usual power flow goes from higher to lower voltage levels, or, in other words, from transmission to distribution grid; DG units, however, could reverse this condition and force power to flow from low voltage toward medium voltage grid. This results in a conflict with the original relay protection calculation scheme, and the intervention of electronic equipments can further reduce the short current value during a fault. So, a proper optimization of reliability and availability of supplied power requires the protection system to be sufficiently selective [9].

These issues are mostly solved by appropriate hardware application and control. The adoption of power converters on load side can for sure improve power quality. In this way, a fault can be restricted only to the place where it has occurred, without compromising other loads on the same grid.

Due to economic reasons, islanding detection, aimed to protect the grid from reverse power flow, cannot be implemented through drastic changes in the protection system. A possible and profitable approach consists in keeping the original relays but adopting different schemes for different network configuration. For each scheme the settings of relays are recalculated, changing maximum and minimum operational limits.

So, it's easy to understand that distribution grids require modern and innovative solutions to solve all these possible sources of disturbances and faults.

In this paper, the authors suggest an advanced methodology to achieve power flow control and optimization on LV distribution systems by means of a low-voltage unified power flow controller (UPFC). The UPFC is made of a combination of a series inverter, a shunt inverter and a dc-link capacitor: the series inverter controls both active and reactive power flows on the distribution line, while the shunt inverter manages an input line voltage and a dc-link voltage [10].

Unified power flow controllers are normally used to gain power flows control in high voltage transmission systems by managing the right values of the impedance, the voltage magnitude and the phase angle. [11-15]

UPFC can perform the functions of the static synchronous compensator (STATCOM or SSSC) and of the phase angle regulator, and also provide additional flexibility by combining some of the classic functions of these controllers [16]. Alternatively, it can also independently control both the real and reactive power flows in the line.

## 2 Low Voltage Distribution Control by UPFC

In the proposed scheme, a LV-UPFC can be used in order to control active and reactive power flowing in two different lines (i.e. called L1 and L2), belonging to parallel paths of a secondary distribution scheme. The proposed scheme comprises two voltage source converters (VSC1 and VSC2): the first one has a shunt connection with the terminal of a L1 line, while the second is connected to both L1 and L2 and provides a fixed phase and magnitude voltage level between them, in order to control line power flows.

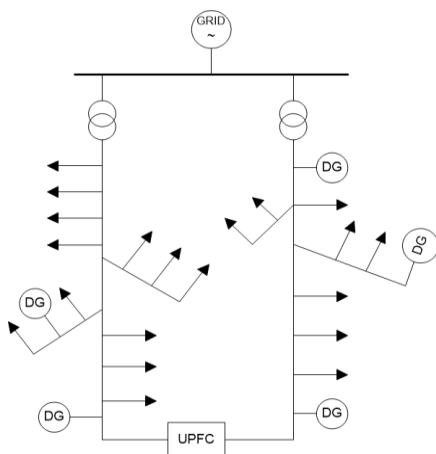


Fig.1 Example of LV grids connected by UPFC

This is possible because the active power injected by VSC2 is balanced by the active power withdrawn by VSC1 and viceversa, while reactive power surged by each VSC is not dependent from the other.

The converters are constituted by three-phase bridges built with IGBT transistors at 10kHz frequency level; the DC link has a voltage level of 800 V and capacity equal to 0,8 mF.

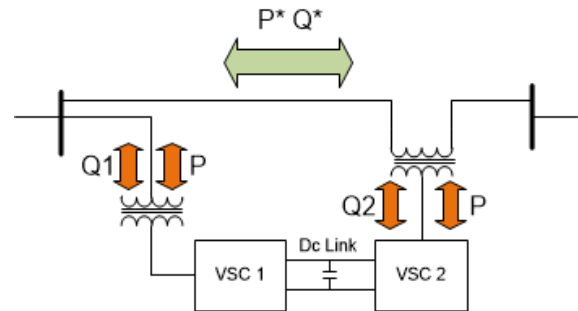


Fig.2 UPFC internal scheme

The converters have two different operating and control schemes.

As shown in Fig. 3, VSC1 is current-controlled by  $I_{ca}$ ,  $I_{cb}$ ,  $I_{cc}$ , which are drained from the L1 terminal. Considering a  $d, q$  rotating coordinate system, the  $d$  axis of the chosen coordinate system is aligned with the grid voltage vector, according the voltage oriented control technique (VOC).  $V_{1\omega}$ ,  $V_{1b}$  and  $V_{1c}$  are referred to the Thevenin equivalent model of the grid calculated in respect to the connection point of VSC1.

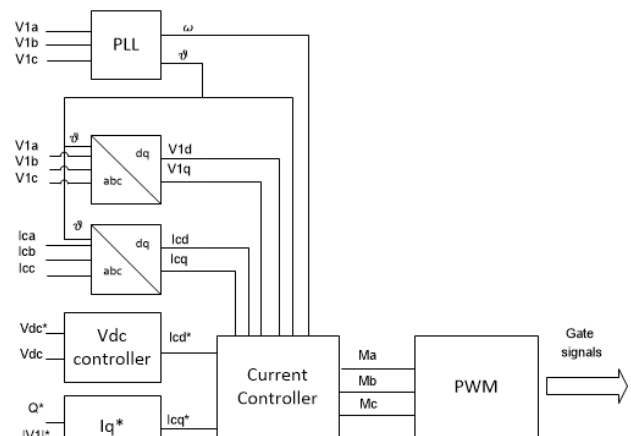


Fig.3 VSC1 control architecture

Figure 4 shows the equivalent circuit of the current controller VSC1. The controller was modeled as a single-phase R-L circuit, where  $L'$  and  $R'$  indicate the total inductance and resistance given by the line transformer and the internal filter of VSC1.

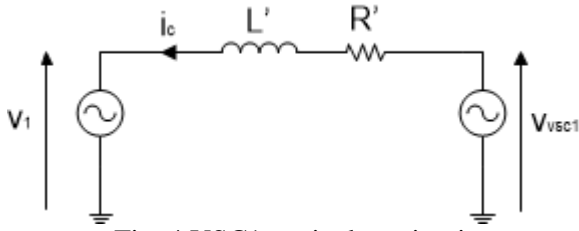


Fig. 4 VSC1 equivalent circuit

Equations used for designing the PI current controllers are:

$$V_{VSC1d} = R' I_{cd} + L' \frac{dI_{cd}}{dt} - \omega L' I_{cq} + V_{1d} \quad (1)$$

$$V_{VSC1q} = R' I_{cq} + L' \frac{dI_{cq}}{dt} + \omega L' I_{cd} + V_{1q} \quad (2)$$

where  $V_{1d}$ ,  $V_{1q}$  indicate the voltages of the converter. The relations between active and reactive power and  $I_{cd}$  and  $I_{cq}$  currents can be written as follows:

$$P = \frac{3}{2} V_{1d} I_{cd} \quad (3)$$

$$Q_1 = -\frac{3}{2} V_{1d} I_{cq} \quad (4)$$

In order to determinate current set point on  $d$  axis, it is necessary to control the DC link voltage  $V_{dc}$ .

There are two external decoupled control loops, that calculate the current set-points for  $I_{cd}^*$  and  $I_{cq}^*$ . The first loop manages the voltage level of the capacitor and determines the active power that the converter exchanges with L1. The second loop determines  $I_{cq}^*$  according two different processes: the equation (4) is applied if the  $Q_1$  value is known; otherwise it is possible to measure  $V$  on L1, compare this value with the voltage set point and finally calculate the  $I_{cq}^*$  set point with a PI controller.

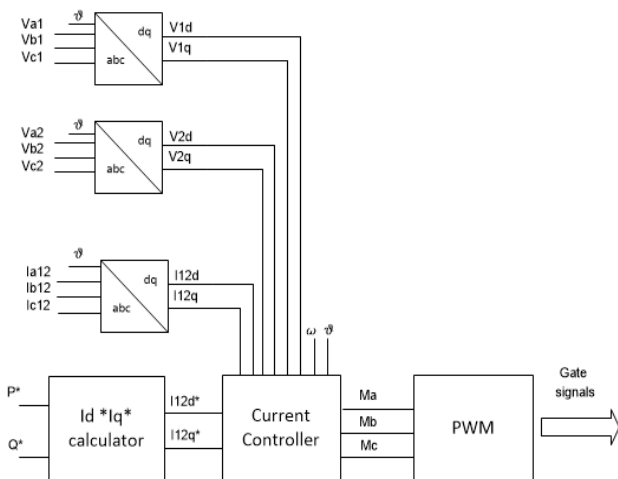


Fig.5 VSC2 control architecture

VSC2 is also current-controlled, but as shown in Figure 5, currents are directly depending from the ones flowing between L1 and L2 ( $I_{a12}$ ,  $I_{b12}$ ,  $I_{c12}$ ). The internal current loop needs the voltage values on L1 and L2 terminals ( $V_{a1}$ ,  $V_{b1}$ ,  $V_{c1}$  and  $V_{a2}$ ,  $V_{b2}$ ,  $V_{c2}$ ).

Figure 6 shows the VSC2 equivalent circuit. In this case  $L''$  and  $R''$  indicate the total inductance and resistance of the internal filter of VSC2;  $V_1$  and  $V_2$  are the voltage levels on L1 and L2 terminals and  $V_{VSC2}$  is the voltage provided by VSC2.

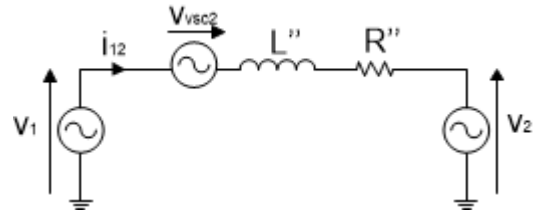


Fig. 6 VSC2 equivalent circuit

The plant equations become now:

$$V_{VSC2d} = R'' I_{12d} + L'' \frac{dI_{12d}}{dt} - \omega L'' I_{12q} + V_{2d} - V_{1d} \quad (5)$$

$$V_{VSC2q} = R'' I_{12q} + L'' \frac{dI_{12q}}{dt} + \omega L'' I_{12d} + V_{2q} - V_{1q} \quad (6)$$

$I_{12d}^*$  and  $I_{12q}^*$  are calculated by (7) equation:

$$\begin{bmatrix} I_{12d}^* \\ I_{12q}^* \end{bmatrix} = \frac{2}{3} \frac{1}{V_{1d}^2 + V_{1q}^2} \begin{bmatrix} +V_{1d} + V_{1q} \\ +V_{1q} - V_{1d} \end{bmatrix} \begin{bmatrix} P^* \\ Q^* \end{bmatrix} \quad (7)$$

$P^*$  and  $Q^*$  star represent the active and reactive power levels that should flow through LINE1 and LINE2; the  $\omega$  pulse and  $\vartheta$  angle values are calculated by the PLL controller. The  $Q_1$  level is always supposed to be equal to zero because our target is not to exchange reactive power through the VSC1 but manage  $P$  and  $Q$  flows between L1 and L2.

### 3 Test Cases

For testing the proposed approach, a low voltage system linked to a 20 kV distribution MV grid was adopted (figure 7).

The MV bus feeds two different transformers, T1 and T2, and their respective lines called L1 and L2. DG units are installed on both lines. Feeder L2 supplies a greater power demand and owns more power capacity installed from distributed generation. The UPFC is supposed to be connected at the back-current feeding switch at end of the two feeders.

Main parameters of transformers and lines are reported in Table 1 and Table 2.

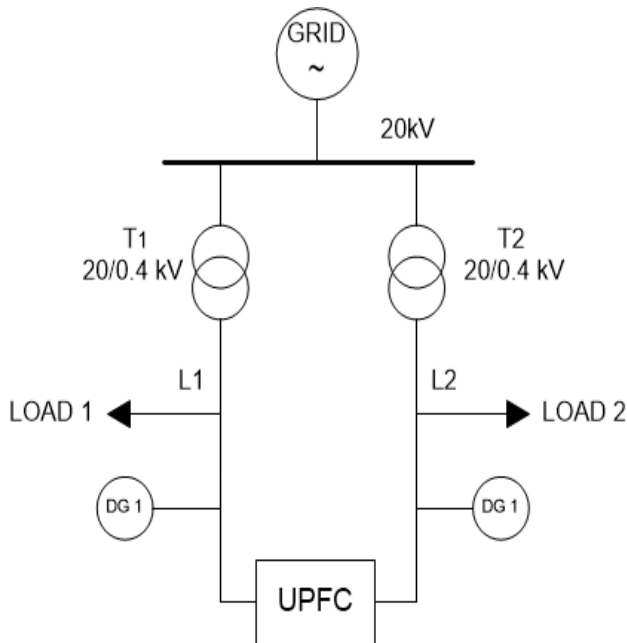


Fig. 7 Grid topology

TABLE 1 Lines parameters

|                    | L1      | L2          |
|--------------------|---------|-------------|
| Length (m)         | 1200    | 400         |
| Cables             | 3x70+50 | 2x3x150+150 |
| R (Ω/km)           | 0,270   | 0,063       |
| X (Ω/km)           | 0,075   | 0,074       |
| I <sub>z</sub> (A) | 215     | 688         |

TABLE 2 Transformers Parameters

|                    | T1        | T2        |
|--------------------|-----------|-----------|
| Voltage ratio (kV) | 20/0,4    | 20/0,4    |
| Connections        | Delta-wye | Delta-wye |
| U <sub>cc</sub> %  | 6         | 4         |
| P <sub>Cu</sub> %  | 1,8       | 1,8       |
| An (kVA)           | 160       | 400       |

In this study three different test have been carried out. In Case 1, the LV-UPFC controls system losses through an optimal distribution of active and reactive power flows in both L1 and L2 feeders, In Case 2, the LV-UPFC aims at controlling counterflows caused by excessive generation located on L1. The third case, Case 3, shows how the controller can be exploited for solving a line congestion problem due to high power demand in L1.

## 4 Numerical Results

### 4.1 Case 1

The initial conditions of the grid for Case 1 are reported in Table 3; UPFC was set so that  $P^*$  and  $Q^*$  flows are equal to zero. In this way the system operates just like there was no connection between the lines. Active power loss was equal to 13 kW. The active and reactive power through T1 and T2 values (including power losses) are reported as “Load 1” and “Load 2”.

TABLE 3 Initial conditions, case 1

| Load / DG | P (kW) | Q (kVAR) | A (kVA) |
|-----------|--------|----------|---------|
| Load 1    | 80     | 20       | 82.46   |
| Load 2    | 30     | 5        | 30.41   |
| DG1       | 20     | 0        | 20,00   |
| DG2       | 10     | 0        | 10,00   |

Next figures show how it is possible to balance power flows distribution and reduce power losses on the lines.

At  $t=0$ , the UPFC started to shift almost 9 kW from L2 to L1 (figure 9). Consequently,  $P$  flowing through T1 decreased from almost 70 to 60 kW, while the active power through T2 increased from 20 to almost 30 kW (figure 10–11). These optimization caused a relevant decrement of power losses on L1 and a total loss reduction of 25% (from more than 13 to about 9.8 kW).

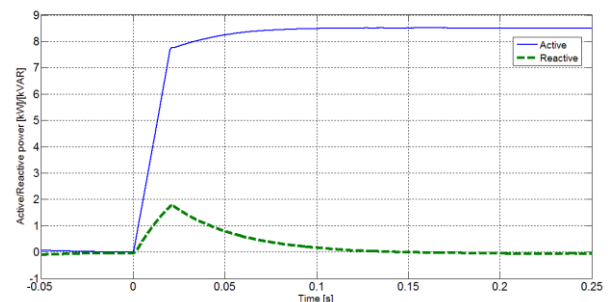


Fig. 9 UPFC power flow – case 1

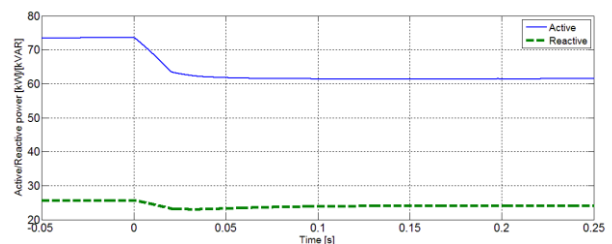


Fig. 10 T1 power flow - case 1

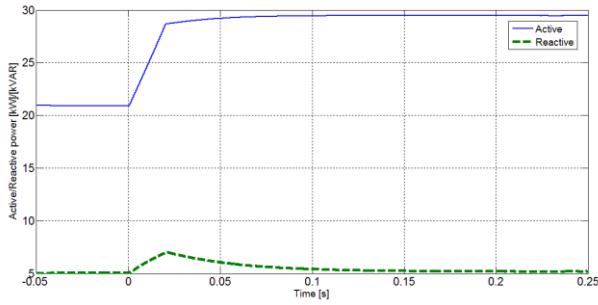


Fig. 11 T2 power flow - case 1

### 4.2 Case 2

In this case the DG unit on L1 was injecting 60 kW on the grid, causing the inversion of power flowing through T1. Assuming as negative power flows going from low voltage to medium, the active power at T1 is -20 kW.

In order to manage flow balance, at  $t=0$  UPFC started to transfer  $P^* = 20$  kW from L1 to L2 (figure 12). Grid configuration is reported in Table 4.

TABLE 4 Initial conditions, case 2

| Load / DG | P (kW) | Q (kVAR) | A (kVA) |
|-----------|--------|----------|---------|
| Load 1    | 40     | 10       | 41,23   |
| Load 2    | 150    | 40       | 155,24  |
| DG 1      | 60     | 0        | 60,00   |
| DG 2      | 50     | 0        | 50,00   |

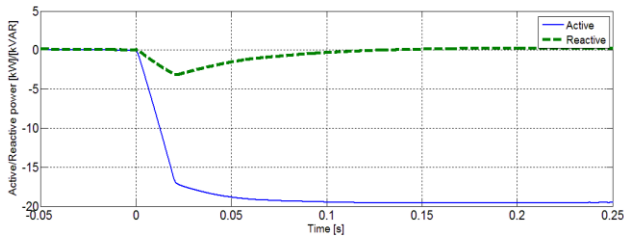


Fig. 12 UPFC power flow - case 2

In Figure 13 it is possible to note how  $I_{a12}$  oscillates between -40 and +40 A after  $t=0$ . In figures 14 and 15 active and reactive flows at the transformers are shown. At  $t=0$ , the UPFC started to transfer  $P^*$  from L1 to L2; consequently,  $P$  provided by T2 increased of almost 20 kW while T1 stopped the injection of the same quantity back toward the MV grid.

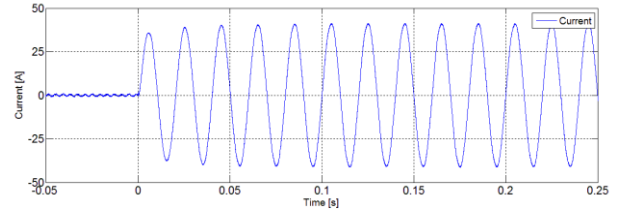


Fig. 13 UPFC current - case 2

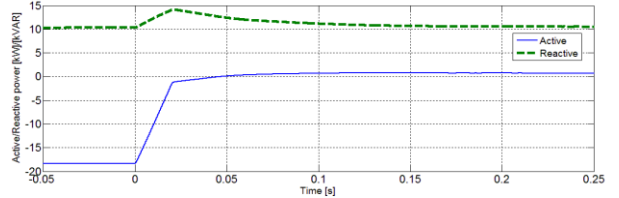


Fig. 14 T1 power flow - case 2

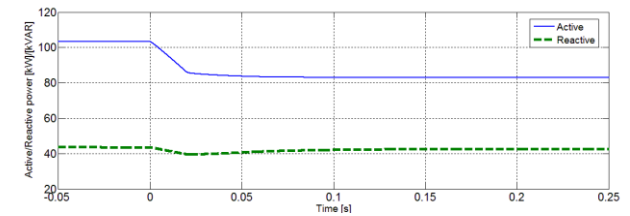


Fig. 15 T2 power flow - case 2

### 4.3 Case 3

The starting conditions for this last case are reported in Table 5. Distributed generation on L1 was null, so the UPFC was used to inject power from L2 in order to prevent a congestion.

TABLE 5 Initial conditions, case 3

| Load / DG | P (kW) | Q (kVAR) | A (kVA) |
|-----------|--------|----------|---------|
| Load 1    | 100    | 0        | 100     |
| Load 2    | 70     | 10       | 70,71   |
| DG 1      | 0      | 0        | 0       |
| DG 2      | 30     | 0        | 30      |

In the following figures we can see as, for  $t=0$ , the UPFC began to shift 15 kW across the two feeders. The active power on L1 decreased from almost 150 to 115 kW. The active power level was so high because of the notable length of L1 that causes additional voltage drop. At the same time, L2 increased from 40 kW (we consider the total  $P$  obtained subtracting distributed generation from load) to 55 kW.

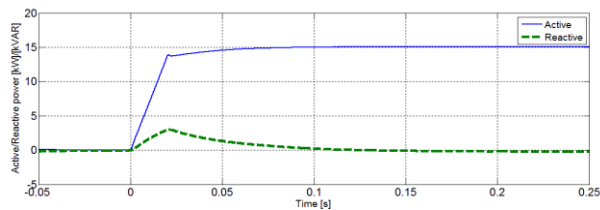


Fig. 16 UPFC power flow – case 3

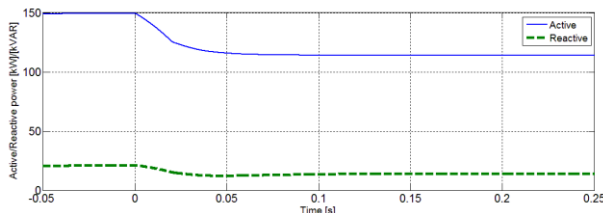


Fig. 17 T1 power flow - case 3

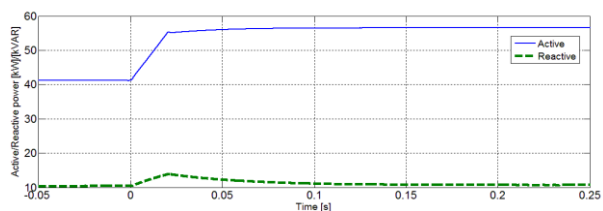


Fig. 18 T2 power flow - case 3

## 5 Conclusions

In this paper, authors presented a methodology aimed to assure power flow control and optimization on low voltage distribution systems by means of a low-voltage unified power flow controller (LV-UPFC). Test cases have been developed to show how these devices can be adopted to solve some typical operative issues in low voltage grids characterized by a wide penetration of DG. The proposed control scheme was tested for controlling power flow inversion, power losses and congestion events.

Future research will be focused on the implementation of advanced mathematical methodologies and efficient algorithms in order to automatically calculate the best set-points of  $P^*$  and  $Q^*$  for UPFC. This will represent a crucial step for increasing the feasibility of future installations of these devices in low voltage smart grids.

*Acknowledgement* - The present study was developed within the framework of the project PON RES NOVAE (Reti, Edifici, Strade, Nuovi Obiettivi Virtuosi per l'Ambiente e l'Energia), supported by the Italian Ministry for Education, University and Research, under the research and competitiveness program to promote "Smart Cities Communities and Social Innovation

## References:

- [1] F. Muzi, "Smart Grids and distributed generation: the future electricity networks of the European Union", *3<sup>rd</sup> IASME/WSEAS Int. Conf. on Energy & Environment*, University of Cambridge, UK, 23<sup>rd</sup> – 25<sup>th</sup> Feb. 2008
- [2] M. Zahran, "Smart Grid Technology, Vision, Management and Control", *WSEAS Trans. on Systems*, vol. 12, issue 1, Jan. 2013
- [3] N. Acharya, P. Mahat, N. Mithulananthan, "An analytical approach for DG allocation in primary distribution network", *Int. Journal of Electric Power Energy System*, vol. 28, no.10, pp. 669-678, Dec. 2006
- [4] M.R. Haghifam, H. Falaghi, O.P. Malik, "Risk-based distributed generation placement", *IET Gener. Transm. Distrib.*, vol. 2, no.2, pp.252-260, Mar. 2008
- [5] S. Kotamarty, S. Khushalani, N. Schulz, "Impact of distributed generation on distribution contingency analysis", *Elect. Power Systems Res.*, vol.78, no.9, pp. 1537-1545, Sep. 2008
- [6] L.F. Ochoa, G.P. Harrison, "Minimizing energy losses: Optimal accommodation and smart operation of renewable distributed generation", *IEEE Transactions on Power Systems*, vol. 26, no.1, pp. 198-205, Feb. 2011.
- [7] N.G.A. Hemdan, M. Kurrat, "Efficient integration of distributed generation for meeting the increased load demand", *International Journal of Electric Power Energy Systems*, vol. 33, no.9, pp. 1572-1583, Nov. 2011
- [8] D.Q. Hung, N. Mithulananthan, "Multiple distributed generators placement in primary distribution networks for loss reduction", *IEEE Trans. Ind. Electron.*, vol. 60, no. 4, pp. 1700-1708, Apr. 2013
- [9] C.X. Wu, F.S. Wen, Y.L. Lou, "The existed problems and possible solutions of micro-grid based on distributed generation", *3<sup>rd</sup> International Conference on Deregulation and Restructuring and Power Technologies DRPT 2008*, 6<sup>th</sup> -9<sup>th</sup> Apr 2008, Nanjing, China.
- [10] D.G. Cho, E. Ho. Song, "A simple UPFC control algorithm and simulation on stationary reference frame", *International Symposium on Industrial Electronics ISIE 2001*, 12<sup>th</sup> – 16<sup>th</sup> June 2001, Pusan, Korea

- [11]J. Joglekar, Y. Nerkar, “Application of UPFC for improving micro-grid voltage profile”, *IEEE International Conference on Sustainable Energy Technologies ICSET* 2010, 6<sup>th</sup> – 9<sup>th</sup> Dec. 2010, Kandy, Sri-Lanka
- [12]Y.M. Alharbi, A.M. Shiddiq Yunus, A. Abu Siada, “Application of UPFC to improve the LVRT Capability of wind turbine generator”, *22<sup>nd</sup> Australasian Universities Power Engineering Conference AUSPEC*, 26<sup>th</sup> – 29<sup>th</sup> Sept. 21012, Bali
- [13]M.A. Sayed, T. Takeshita, “Line loss minimization in isolated substations and multiple loop distribution systems using UPFC”, *IEEE Transactions on Power Electronics*, Volume PP, Issue 99, Jan. 2014
- [14]V. Uma, P. Lakshmi, J. D. Anunciya, “Congestion management in deregulated power systems by fuzzy based optimal location and sizing of UPFC”, *WSEAS Trans. on Power Systems*, pp. 258 – 266, vol. 9, 2014
- [15]I. Musirin, Nur D. M. Radzi, M. M. Othman et al, “ Voltage profile improvement using unified power flow controller via Artificial Immune System”, *WSEAS Trans. On Power Systems*, issue 4, vol. 3, pp. 194-204, Apr. 2008
- [16]T. Nireekshana, G. Kesava Rao, S. Siva Naga Raju, “Modeling and control design of unified power flow controller for various control strategies”, *International Journal of Engineering Science and Technology*, vol. 2, pp. 6293-6307, 2010